The deafness gene *dfna5* is crucial for *ugdh* expression and HA production in the developing ear in zebrafish

Elisabeth Busch-Nentwich[1], Christian Söllner[1], Henry Roehl[2] and Teresa Nicolson[3,*]

[1]Max-Planck-Institut für Entwicklungsbiologie, Spemannstr. 35, 72076 Tübingen, Germany
[2]Centre for Developmental Genetics, Department of Biomedical Science, University of Sheffield, Firth Court, Sheffield S10 2TN, UK
[3]Oregon Hearing Research Center and Vollum Institute, Oregon Health & Science University, Portland, OR 97201, USA
*Author for correspondence (e-mail: nicolson@ohsu.edu)

Accepted 30 October 2003

Development 131, 943-951
Published by The Company of Biologists 2004
doi:10.1242/dev.00961

Summary

Over 30 genes responsible for human hereditary hearing loss have been identified during the last 10 years. The proteins encoded by these genes play roles in a diverse set of cellular functions ranging from transcriptional regulation to K^+ recycling. In a few cases, the genes are novel and do not give much insight into the cellular or molecular cause for the hearing loss. Among these poorly understood deafness genes is *DFNA5*. How the truncation of the encoded protein DFNA5 leads to an autosomal dominant form of hearing loss is not clear. In order to understand the biological role of Dfna5, we took a reverse-genetic approach in zebrafish. Here we show that morpholino antisense nucleotide knock-down of *dfna5* function in zebrafish leads to disorganization of the developing semicircular canals and reduction of pharyngeal cartilage. This phenotype closely resembles previously isolated zebrafish craniofacial mutants including the mutant *jekyll*. *jekyll* encodes Ugdh [uridine 5′-diphosphate (UDP)-glucose dehydrogenase], an enzyme that is crucial for production of the extracellular matrix component hyaluronic acid (HA). In *dfna5* morphants, expression of *ugdh* is absent in the developing ear and pharyngeal arches, and HA levels are strongly reduced in the outgrowing protrusions of the developing semicircular canals. Previous studies suggest that HA is essential for differentiating cartilage and directed outgrowth of the epithelial protrusions in the developing ear. We hypothesize that the reduction of HA production leads to uncoordinated outgrowth of the canal columns and impaired facial cartilage differentiation.

Key words: *dfna5*, Deafness, Zebrafish, Semicircular canals, Pharyngeal cartilage, UDP-glucose dehydrogenase, Hyaluronic acid

Introduction

Deafness is one of the most common hereditary diseases (reviewed by Petit et al., 2001; Morton, 2002). One out of 1000 children suffers from congenital deafness and inherited progressive hearing loss affects another 2.5% of the population. Late onset age-related hearing loss is thought to be due to a combination of genetic and environmental causes. To date, over 500 syndromic deafness loci have been identified which confer hearing loss in association with defects in other organ systems (Gorlin et al., 1995). The most common forms of syndromic deafness cause abnormalities in craniofacial and skeletal structures (Branchio-oto-renal syndrome, Stickler syndrome), retinitis pigmentosa (Usher syndrome) or heart defects (Jervell and Lange-Nielsen syndrome) (Abdelhak et al., 1997; Ahmad et al., 1991; Bitner-Glindzicz and Tranebjaerg, 2000; Petit, 2001). In addition, over 90 loci for non-syndromic hearing loss have been identified thus far. For more than 30 of these loci, the affected gene is known (Morton, 2002). In many cases, these genes are responsible for both syndromic and non-syndromic deafness, depending on the nature of the mutation (Astuto et al., 2002).

DFNA5 is a non-syndromic autosomal dominant form of progressive hearing loss that was identified in an extended Dutch family (van Camp et al., 1995; DeLeenheer et al., 2002). High frequency hearing loss starts in the first or second decade of life. The patients carry a complex intronic insertion/deletion mutation that leads to truncation of the protein (Van Laer et al., 1998). *DFNA5* encodes a protein of 496 amino acids that is found in human cochlea, brain, placenta and kidney cDNA preparations. DFNA5 is a novel protein, sharing no obvious homology to other proteins, and as there is no animal model, nothing is known about its molecular function or what role it plays during vertebrate development. To gain insight into a possible function for Dfna5, we examined its expression pattern in developing zebrafish embryos and its function using a morpholino knock-down strategy. Our phenotypic analysis suggests that Dfna5 function is essential for development of the semicircular canals and the pharyngeal cartilage, and acts at the level of extracellular matrix production.

The extracellular matrix plays an important role in cell migration, differentiation and morphogenesis of organs such as the ear and jaw. The ear and the pharyngeal cartilage arise from the same region of the embryo. In zebrafish, the otic placode develops from the cells overlying the second cranial neural crest (CNC) stream, adjacent to rhombomeres 5 and 6, at about 14 hpf (hours post fertilization). At around 45 hpf, the

epithelial projections of the developing semicircular canal begin to grow out. At 52 hpf, the opposing projections of the anterior and posterior canals touch and fuse. This process is completed with the fusion of the ventral column at 64 hours. The directed outgrowth of the protrusions is dependent on secretion of extracellular matrix (ECM), including hyaluronic acid (HA), into the extending lumen between the epithelium and the underlying mesenchyme (Haddon and Lewis, 1991). The ECM is later replaced by invading fibroblasts. (Haddon and Lewis, 1991; Haddon and Lewis, 1996; Waterman and Bell, 1984).

The cartilage that gives rise to the jaw and gills is called pharyngeal cartilage and is of neural-crest origin (Schilling and Kimmel, 1994). Pharyngeal cartilage is derived from three streams of cranial neural crest (CNC) that begin to migrate at 12 hpf. The most anterior two CNC streams give rise to the cartilage of the upper and lower jaw, and the posterior stream is subdivided by endodermal pouches to give rise to the five sets of branchial (gill) cartilage. The pharyngeal cartilage condensations begin to differentiate starting at 53 hpf as seen by Alcian Blue staining (reviewed by Kimmel et al., 2001; Schilling and Kimmel, 1994). The early steps of jaw development are regulated by Sox9, under the control of bone morphogenetic proteins (BMPs) and sonic hedgehog (Shh) (de Crombrugghe et al., 2001). After condensation, the differentiating chondrocytes begin to express *col2a1*, the main collagen of differentiated cartilage, *col11a2*, *aggrecan* and other ECM proteins under the control of Sox5 and Sox6. In differentiated cartilage, only 5% of the volume is occupied by chondrocytes, with the remainder consisting of ECM.

Not surprisingly, many genes expressed in the posterior region of the head regulate the development of both the ear and pharyngeal cartilage. For example, expression of *fgf3* and *fgf8* in rhombomere 4 is required for induction of the ear placode and formation of branchial cartilage (Maroon et al., 2002; Leger and Brand, 2002; Liu et al., 2003). A mutation in another gene, *jekyll*, leads to interrupted ear columns and a lack of cranial cartilage (Neuhauss et al., 1996). *jekyll* encodes Udgh, an enzyme required for synthesis of proteoglycans including HA (Walsh and Stainier, 2001). We show that a knock-down of *dfna5* function in zebrafish causes the loss of *ugdh* expression and reduction of HA levels, leading to malformation of the semicircular canals of the ear and pharyngeal cartilage.

Materials and methods

Cloning and physical mapping

We blasted HsDFNA5 protein sequence against EST data from GenBank and obtained an EST clone containing full-length zebrafish *dfna5* cDNA sequence (Accession Number: BE015795). The forward primer 5′-TTGCAAAAGCCACTAAGAACC-3′ and reverse primer 5′-ATCGGTTACGCTTGATGACC-3′ were used on the T51 radiation hybrid panel to physically map zebrafish *dna5* to linkage group 16.

We analyzed the genomic organization of zebrafish *dfna5* partially by blasting the cDNA sequence against genomic zebrafish sequence and partially by PCR on genomic sequence with subsequent cloning and sequencing of the obtained PCR-products.

Whole-mount in situ hybridization

We amplified full-length *dfna5* using the forward primer A5-bf 5′-AGCACGAGCTGATCCTCAAA-3′ and reverse primer A5-br 5′-AAGCCTCGTCTGTTTCGTGC-3′, cloned the 1990 bp fragment and used it as a template to synthesize a digoxigenin labeled in situ RNA probe. For *col2a1* we used the forward primer 5′-CTGGATCT-GATGGTCCACCT-3′ and reverse primer 5′-ACATGGCTGGATT-TCAGAGG-3′ to amplify a 1593 bp fragment and for *ugdh* the forward primer 5′-GACGTACGGTATGGGCAAAG-3′ and reverse primer 5′-TTGATTTCCAGCAATGGTCA-3′ to amplify a 1304 bp fragment. Both PCR-product were used as described for the *dfna5* in situ probe. Whole-mount in situ hybridization was performed as described previously (Thisse et al., 1993).

Antisense morpholino oligonucleotide and DNA injections

We designed one antisense morpholino oligonucleotide (MO, Gene Tools) directed against the 5′ sequence around the putative start codon to block *dfna5* translation (“ATG-MO”) and one MO against the splice donor site of exon 8 to interfere with splicing (“GT-MO”). The sequences for the ATG-MO and the GT-MO were 5′-TGCAAAC-ATCTTCAATGCTGACAAG-3′ and 5′-TGATTTAACTGAACTCA-CCGTCTAG-3′, respectively. An additional morpholino with four base pair exchanges was designed for control injections. The sequence for the mismatch MO was 5′-TGCGAACACCTTTAATGCTAAC-AAG-3′. We injected concentrations between 10 and 40 ng in single cell embryos in a volume of 5 nl.

For rescue experiments we amplified full-length *dfna5* with the primers used for generation of the in situ probe template, cloned it in pCS2+ vector and identified a mutation free clone by sequencing. The plasmid was co-injected in single cell embryos with different concentrations of ATG-MO in a concentration of 50 pg/nl.

Histology and electron microscopy

Whole larvae (day 5) were anesthetized with 0.02% MESAB (3-aminobenzoic acid ethyl ester) and then fixed in 2.0% glutaraldehyde and 1.0% paraformaldehyde in PBS overnight to several days at 4°C. Specimens were fixed with 1.0% OsO_4 in H_2O for 10 minutes on ice, followed by fixation and contrast with 1.0% uranyl acetate for 1 hour on ice, and then dehydrated with several steps in ethanol and embedded in Epon. Sections (5 μm) were stained with Toluidine Blue. Ultrathin sections were stained with lead citrate and uranyl acetate.

Alcian-Blue cartilage staining

Cartilage was stained with Alcian Blue as described previously (Schilling et al., 1996).

Whole mount labeling for hyaluronic acid

Freshly fixed larvae (4% PFA in PBS overnight at 4°C) were permeabilized for 6 hours at room temperature with 2% Triton, 4% PFA in PBS. After washing several times in TBS, larvae were incubated with 10 μg/ml biotinylated hyaluronic acid binding protein (HABP) from Seikagaku corporation in TBS overnight at 4°C. The HABP was removed and the larvae washed in TBS three times for 20 minutes. After 4 hours blocking with 2% BSA in TBS at room temperature, the larvae were incubated with anti-biotin rabbit antibody (Heinz Schwarz, Tübingen), diluted 1:50 in TBS for 3 hours at room temperature. The larvae were washed in TBS three times for 20 minutes and incubated overnight at 4°C with alexa-Fluor-coupled anti-rabbit antibody, diluted 1:500. After rinsing several times, larvae were mounted on a glass slide in 1.5% low melting point agarose and examined.

Results

Sequence analysis and expression of *dfna5*

To explore the function of *dfna5* in vertebrates, we cloned the zebrafish orthologue of *DFNA5* by blasting the human protein sequence against EST databases. Zebrafish Dfna5 has 472 amino acids with 33% identity and 51% similarity to human

Fig. 1. Protein alignment of zebrafish, human and mouse Dfna5. Black shading indicates identity and gray shading indicates similarity. The overall identity of zebrafish compared with human and mouse Dfna5 is 33% and 30%, respectively. Similarity of zebrafish compared with human and mouse Dfna5 is 51% and 49%, respectively.

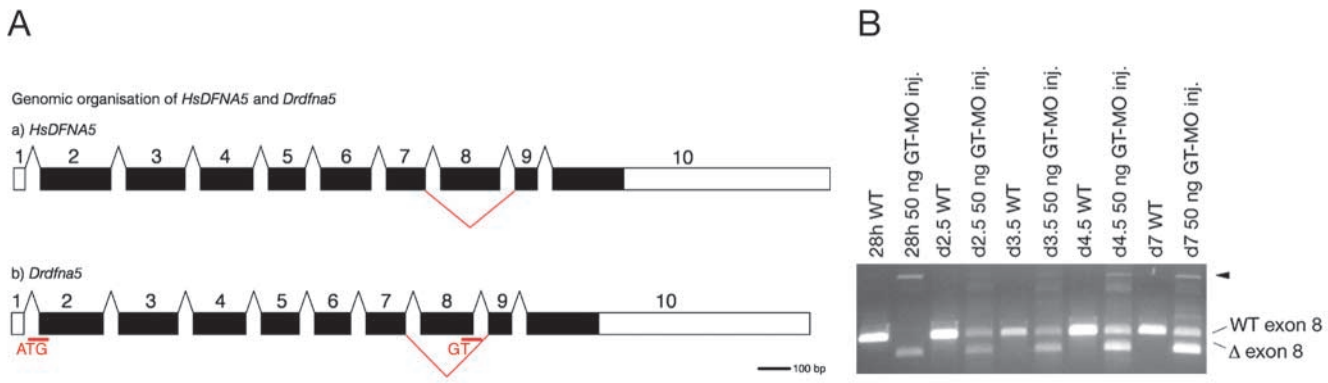

Fig. 2. Target sites of the *dfna5* morpholinos and aberrant splicing of *dfna5* transcript. (A) Genomic organization of human DFNA5 and zebrafish Dfna5. The exon/intron boundaries of *DFNA5* are entirely conserved between human and zebrafish. (a) Individuals with *DFNA5* mutations carry an insertion/deletion mutation in intron 7, which leads to skipping of exon 8 (indicated in red). Absence of exon 8 causes a frameshift after amino acid 330, resulting in an aberrant stretch of 41 amino acids followed by a premature stop. (b) The two morpholino antisense oligos designed against *Dfna5* mRNA are indicated in red. The splice site antisense oligo ('GT-MO') directed against the donor site of exon 8 leads to skipping of the targeted exon (indicated in red), resembling the human mutation. (B) RT-PCR time course of aberrant splicing of *dfna5* mRNA caused by the *dfna5* GT-MO. At 28 hpf, wild-type *dfna5* transcript is not detectable by RT-PCR, only PCR products lacking exon 8 (indicated with Δ exon 8) or with partial retention of the following intron (arrowhead) are present. Wild-type transcript recovers starting at day 2, but the morpholino-modulated transcripts are still present at day 7.

DFNA5 with 496 amino acids (Mouse Dfna5 values are 30% and 49%, respectively) (Fig. 1). With respect to genomic organization, the human and zebrafish genes are highly conserved (Fig. 2A). Both genes have ten exons with identical exon/intron boundaries. The first exon in each gene encodes a short 5′UTR of about 40 bp, and the last exon contains the 3′ end of the open reading frame and a large 3′UTR of about 680 bp.

The temporal and spatial expression pattern of *DFNA5* has not been determined. We carried out in situ hybridization to establish where *dfna5* is expressed in the zebrafish. At stages earlier than 20 hpf, *dfna5* is weakly expressed in a ubiquitous fashion (data not shown). At 20 hpf, it is expressed in the intermediate cell mass, the olfactory placode, the ventral diencephalon and the CNC (Fig. 3A,B). At 48 hpf, *dfna5* mRNA is present in the brain and in the ear, predominantly in the projections of the developing semicircular canals (Fig. 3C). At 55 hpf, expression in the brain decreases, whereas it is elevated in the ear projections (Fig. 3D,F). We detected *dfna5* mRNA at very low levels in the fused ear columns and the brain at 72 hpf (Fig. 3E). At later stages, *dna5* mRNA was no longer detectable (data not shown). A sense probe did not produce a signal at any stage (data not shown).

A splice site morpholino directed against exon 8

Individuals with a mutation in *DFNA5* carry a complex insertion/deletion mutation on chromosome 7p15 in intron 7 of *DFNA5*, which leads to skipping of exon 8 (Fig. 2A, part a, red), causing a premature stop codon after an aberrant stretch of 40 additional amino acids (Van Laer et al., 1998). In order to target the same exon affected in the human disease, we designed a morpholino directed against the donor site ('GT-MO') of exon 8 in zebrafish *dfna5* (Fig. 2A, part b, red). Blocking the donor site of an exon can cause skipping of the targeted exon and/or partial retention of the intron. We traced efficiency of the *dfna5* GT-MO by RT-PCR with primers flanking the targeted exon on wild type and GT-MO injected embryos at different time-points (Fig. 2B). RT-PCR on RNA from 28 hpf GT-MO-injected embryos produced only PCR products that lacked exon 8 (Fig. 2B, indicated with Δ exon 8)

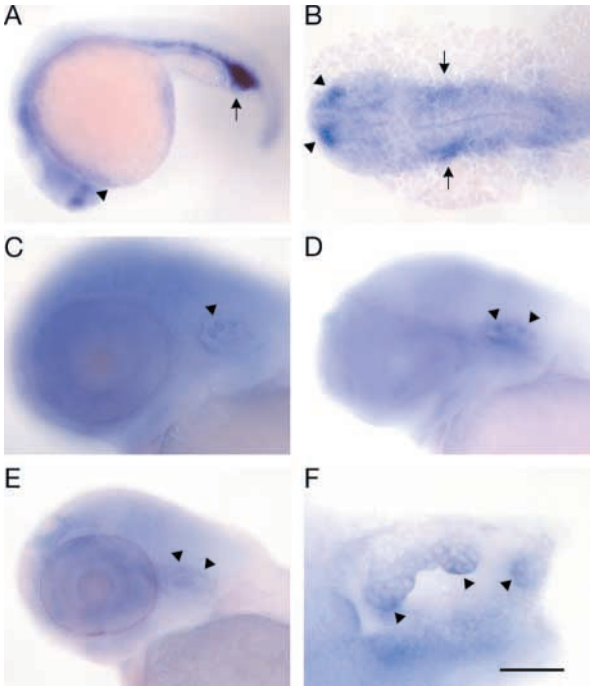

Fig. 3. Expression of *dfna5* in zebrafish embryos using whole-mount in situ hybridization. (A,B) 22 hpf embryo. Lateral (A) and dorsal view of the head region (B), showing expression in the intermediate cell mass (arrowhead in A), the olfactory placodes (arrows), ventral diencephalon and migrating neural crest (arrows in B). (C,D) 48 hpf embryo (C) and 55 hpf embryo (D) with expression in the developing semicircular canals of the ear (arrowheads). (E) 72 hpf embryo indicating low level of expression in the mature projections of the semicircular canals in the ear (arrowheads). (F) Dorsal view of the ear at 48 hpf with expression at the tip of the outgrowing projections of the semicircular canals (arrowheads). Scale bar: 300 μm in A,B; 100 μm in C-E; 40 μm in F.

or partially retained the downstream intron (Fig. 2B, arrowhead). Recovery of wild-type *dfna5* message started at 48 hpf, but as late as day 7 the GT-MO modulated mRNAs were still detectable. Sequencing of the PCR product lacking exon 8 showed that the loss of exon 8 did not cause a frameshift in the *dfna5* mRNA. A second morpholino was designed against the start codon to block translation of the mRNA ('ATG-MO') and thereby knock down the full-length gene.

Knock-down of *dfna5* leads to ear and jaw malformation

To determine the function of *dfna5* in zebrafish, we analyzed the phenotype in animals injected with either ATG or GT *dfna5* morpholinos. Injection of the ATG-MO (Fig. 4) or the GT-MO caused malformation of the semicircular canals of the ear. Either anterior, posterior or both columns of the developing semicircular canals were not fused (Fig. 4E,G,I). At higher doses the lateral canal also did not form (Fig. 4J). The projections, which grow out and fuse to form the columns, were present, but short and thickened. Other structures of the ear, like the cristae or maculae, were unaffected.

With increasing ATG-MO dose, starting at 7.5 ng, we saw an additional phenotype, namely a deformation of the ventral jaw. Injections of 15 ng of ATG-MO (Fig. 4B) resulted in a mildly affected, smaller ventral jaw; 25 ng of ATG-MO led to a severely malformed jaw (Fig. 4C). Meckel's cartilage was ventrally displaced, leading to a widely opened mouth. This phenotype, unfused ear columns and malformed jaw, is similar to the phenotype seen in a particular class (Group II) of zebrafish cartilage differentiation and morphogenesis mutants (Neuhauss et al., 1996). At doses higher than 30 ng, we obtained unspecific side effects such as heart edema with the

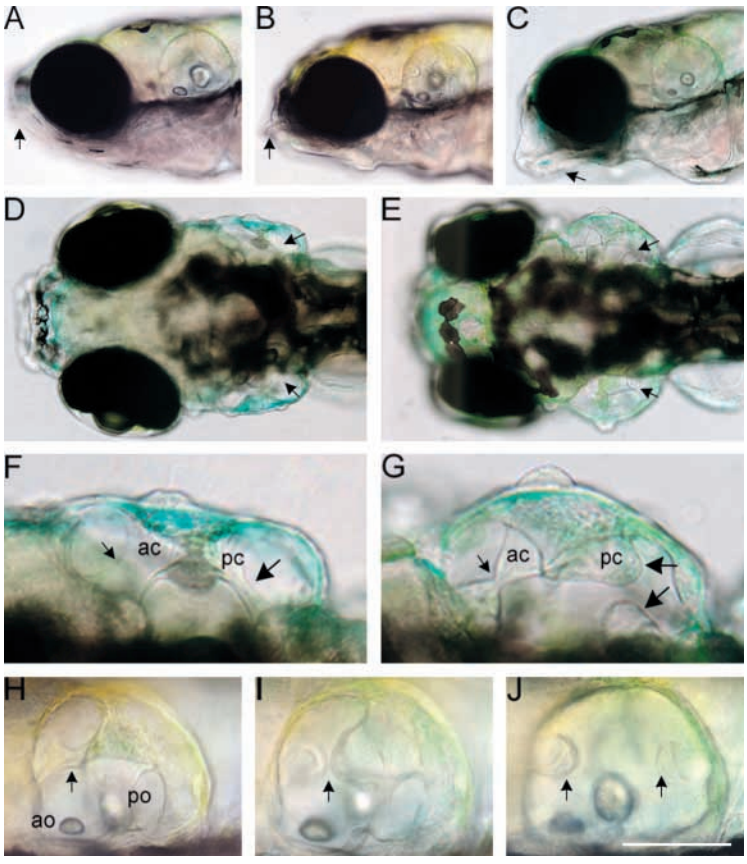

Fig. 4. Reduction of *dfna5* activity leads to abnormal ear and cartilage development. (A-C) Lateral views of wild-type (A), 15 ng *dfna5* ATG-MO-injected (B) and 25 ng *dfna5* ATG-MO-injected (C) embryos, indicating a dose-dependent malformation of the lower jaw (arrows). (D,E) Dorsal view of wild-type (D) and 20 ng dfna5 ATG-MO-injected (E) embryos at day 5, showing malformation of the anterior and posterior column in the morphant ear (arrows). (F,G) Close up of the right ear in D and E, respectively. (G) The anterior column (ac, arrow) of the morphant is malformed, the posterior column (pc, large arrows) is interrupted. (H-J) Lateral view of the ear at day 5 (anterior towards the left, ventral towards the bottom) of wild type (H), 15 ng *dfna5* ATG-MO injected (I) and 25 ng *dfna5* ATG-MO injected (J) embryos. In morphants, either one or more columns do not fuse (arrows), depending on the injected dose of *dfna5* ATG-MO. ao, anterior otolith; po, posterior otolith. Scale bar: 300 μm in A-C; 250 μm in D,E; 80 μm in F,G; 125 μm in H-J. ac, anterior column; pc, posterior column.

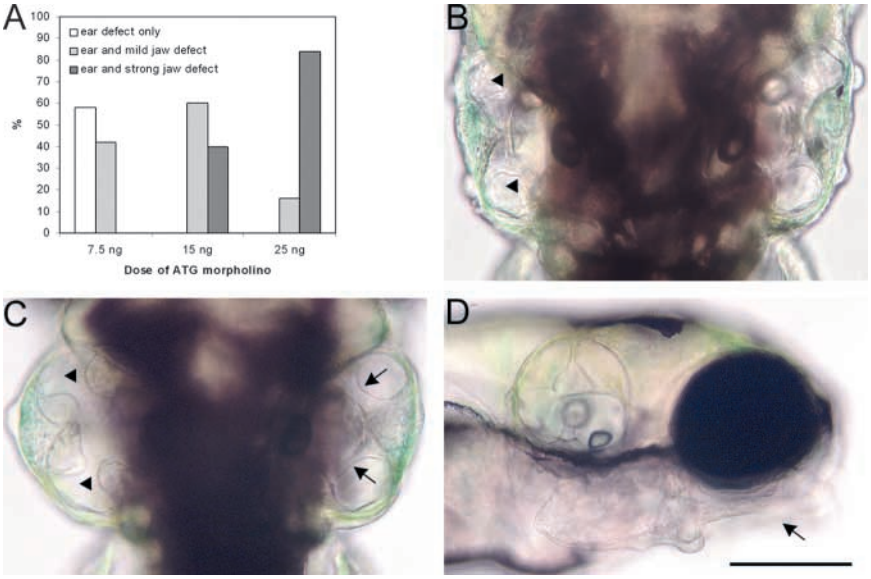

Fig. 5. Specificity of the ATG morpholino-induced phenotype. (A) Dose dependency of the observed phenotype. (B) Injection of up to 25 ng 4 bp mismatch morpholino does not cause any mutant phenotype. (C,D) Partial rescue of the morphant phenotype by co-injection of *dfna5* DNA. Dorsal (C, anterior towards the top) and lateral (D, anterior towards the right) view of one d5 larva injected with 25 ng *dfna5* ATG-MO and 70 pg *dfna5* pCS2+. Left ear (C) and jaw (D) show malformations typical for injections of relatively high doses of ATG-MO, whereas the right ear is rescued and shows no morphological abnormalities. The anterior and posterior columns are properly fused, which is never observed in larvae injected with 25 ng ATG-MO only. Scale bar: 130 μm in B,C; 200 μm in D.

ATG-MO (data not shown). In fish injected with the GT-MO (20 ng-30 ng), we observed only the ear phenotype. A mild jaw phenotype in addition to the ear malformation (but no unspecific effects) was obtained with very high doses (40 ng, data not shown), suggesting that the GT-MO phenotype represents a hypomorphic situation.

As *dfna5* mRNA is highly expressed in the intermediate cell mass which gives rise to blood cells, we analyzed this tissue in more detail. We did not see any change in expression of *scl*, an early blood marker (data not shown). In addition, staining of blood cells with o-dianisidine did not reveal any differences (data not shown).

To exclude the possibility that toxicity of injecting high amounts of morpholino led to the jaw and ear phenotype, we examined cell death in MO-injected animals. Embryos injected with two different doses of ATG-MO (20-40 ng) were stained with Acridine Orange at 35 hpf and 48 hpf. We did not observe elevated levels of cell death in any tissue compared with uninjected embryos (data not shown).

We observed a strong correlation between the amount of MO injected and the resulting phenotype, indicating the specificity of the morpholino knockdown of *dfna5* (Fig. 5A). In addition, injection of a 4 bp mismatch control oligonucleotide did not produce any effects on ear or jaw development (Fig. 5B). To gain further evidence of specific interference with *dfna5* function, we co-injected *dfna5* ATG-MO with an expression construct containing the full-length coding sequence of *dfna5* under the control of the cytomegalo virus (CMV) promoter into one cell-stage wild-type embryos. We found a partial rescue of the phenotype (Fig. 5C,D) at day 5 in 20% of the embryos with strongly affected ears and jaw (n=20). In partially rescued larvae, one ear and the lower jaw showed severe malformations typical for injection of high doses of ATG-MO, whereas the other ear was completely normal. A partial rescue was expected because of the highly mosaic expression of injected DNA. Injection of ATG-MO alone never led to the above 'rescued' phenotype of abnormal jaw morphology combined with normal ear morphology. Only low doses of ATG-MO or GT-MO yielded defects in one ear accompanied by normal morphology in the other ear. However, this unilateral defect was never present in combination with a jaw defect, as seen in larvae co-injected with the expression construct.

dfna5 is essential for development of the inner ear epithelial columns and pharyngeal cartilage

We examined both thick and ultrathin sections of day 5 larval ears to analyze the morphant phenotype in the columns of the ear at the cellular level. We stained 5 μm cross-sections of the lateral canal of the ear at day 6 with Toluidine Blue to visualize nuclei and membranes (Fig. 6A,B). We detected two major defects in the GT-MO injected embryos compared with wild-type embryos. First, the epithelial monolayer of the developing semicircular canal is disrupted (Fig. 6B, arrows). The cells appear to be stretched in an apicobasal direction as opposed to the rather round cells of the wild-type epithelium. In addition, the cells leave the layer and form stacks, which is never observed in the mature wild-type column. Second, the basal lamina of the epithelium is missing or disorganized. In the Toluidine Blue-stained sections, the basal lamina appears in the wild type as a thick blue stripe running down the lateral column (Fig. 6A, arrowhead). In morphant sections, we saw only a few faint light blue lines (Fig. 6B, arrowhead). TEM sections revealed that the basal lamina is composed of parallel, densely packed fibers (Fig. 6C). The morphant basal lamina consists of much fewer and disorganized fibers, which do not run parallel to the epithelial sheet, but point in all directions (Fig. 6D).

The zebrafish larval head skeleton can be divided into four parts, the neurocranium, the mandibular, the hyoid and the branchial cartilage (Schilling and Kimmel, 1997). We used Alcian Blue staining to determine which of these elements are affected in *dfna5* ATG-MO-injected larvae. At day 5, the neurocranium (ethmoid plate, trabeculae, and the anterior and posterior basicranial commissures) is largely unaffected in morphant embryos (Fig. 7A,B). The most obvious defect in the lateral view is the ventrally displaced Meckel's cartilage, which leads to the 'screamer' phenotype (Fig. 7B). The ventral view reveals that although the branchial cartilage is present, the

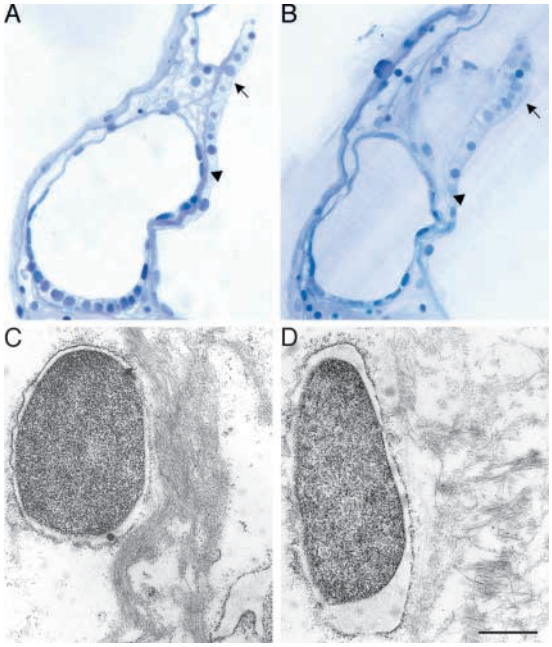

Fig. 6. Histological analysis of the inner ear epithelial columns in *dfna5* morphants. Cross-sections of lateral semicircular canals at day 6 of wild-type (A,C) and *dfna5* GT-MO injected (B,D) embryos. (A,B) Toluidine Blue staining of 5 μm sections, indicating a loss of the monolayer of the epithelium (A,B, arrow) and the basal lamina (A,B, arrowheads) in morphants (B) compared with wild type (A). (C,D) Structure of the basal lamina in TEM cross-sections. (C) The wild-type lamina has tightly packed, parallel fibers. (D) *dfna5* morphant basal lamina is disrupted with loose, disorganized fibers. Scale bar: 20 μm in A,B; 1 μm in C,D.

cartilage from branchial arches 1-4 is strongly reduced (Fig. 7D,E, indicated with 1-4). The cells of the ceratobranchials are irregularly arranged as opposed to the penny stack-like ordered cells in wild-type larvae (Fig. 7C). The basibranchial cartilage is also strongly reduced in size, which most likely leads to the posterior displacement of the ceratohyal cartilage (Fig. 7E, labeled with 2).

The jaw phenotype in *dfna5* morphants indicated a potential defect within the ECM. To determine whether ECM proteins such as collagen were affected in the *dfna5* morphants, we examined the expression of *col2a1*, a marker for differentiating cartilage. At 55 hpf, *col2a1* is expressed at equal levels in wild-type (Fig. 8A) and morphant (Fig. 8D) embryos in the otic vesicle. In contrast to the developing ear, *col2a1* expression was strongly reduced in the developing pharyngeal cartilage (Fig. 8D), suggesting a defect in differentiation.

A previously identified zebrafish mutant that shows a striking similarity to the *dfna5* morphants is the *jekyll* (*jek*) mutant. The ear in *jek* shows a phenotype very similar to *dfna5* morphants. The overall structure and size of the ear is normal. However, although the protrusion of the developing canals form, they fail to elongate and do not fuse (Neuhauss et al., 1996). In addition, *jek* larvae show a strong reduction of all cartilage in the head. *jek* encodes Udgh, an enzyme required for synthesis of proteoglycans including HA. It catalyzes the formation of glucuronic acid, which (together with N-acetylglucosamine) forms the repeating disaccharide unit of hyaluronic acid. To characterize the relationship between *jek/udgh* and *dfna5*, we examined the expression of *ugdh* in *dfna5* morphants. At 55 hpf, *ugdh* is highly expressed in the epithelial columns in the otic vesicle and pharyngeal arches of the jaw in wild-type embryos (Fig. 8B). In *dfna5* morphants, *ugdh* expression is absent in the otic vesicle and pharyngeal arches (Fig. 8E,F). Expression in the developing trabeculae and ethmoid plate is, however, normal (arrows in Fig. 8C,F). This is consistent with the finding that the neurocranium is unaffected in *dfna5* morphants.

Hyaluronic acid levels are strongly reduced in *dfna5* morphants

The biosynthesis of HA depends upon the activities of a number of enzymes, including Ugdh. We tested whether the loss of *ugdh* in the developing semicircular canals affected the production of HA in these structures. We examined the levels of HA in vivo using a biotinylated HA-binding protein (Fig. 9). As shown in Fig. 9C, HA is highly abundant in the semicircular projections of 54 hpf wild-type larvae. Morphant embryos, however, have reduced levels of HA in the protrusions (Fig. 9D-F). This strongly suggests that reduced HA levels lead to the failure of semicircular canal formation in the ear and supports previous findings that HA is important for projection outgrowth.

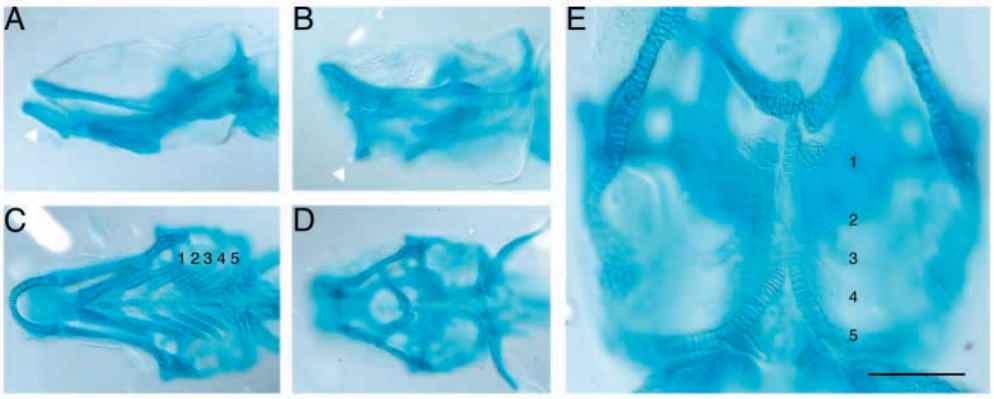

Fig. 7. Abnormal jaw development in *dfna5* morphants. (A-E) Alcian Blue staining of cartilage. (A,C) Lateral (A) and ventral (C) view of a day 5 wild-type larval head. (A) Meckel's cartilage is indicated with a white arrowhead. In C, the ceratobranchials are indicated with 1-5. (B,D,E) Lateral (B) and ventral (D,E) view of a day 5 morphant larval head. (B) Meckel's cartilage (arrowhead) is malformed and the ceratohyal cartilage is inverted, most probably owing to reduction of the branchial cartilages. (E) Cartilage derived from brachial arches 1-5 are present, but strongly reduced. The ceratobranchial cartilage in morphants is less intensely stained than in wild-type. Scale bar: 125 μm in A-D; 200 μm in E.

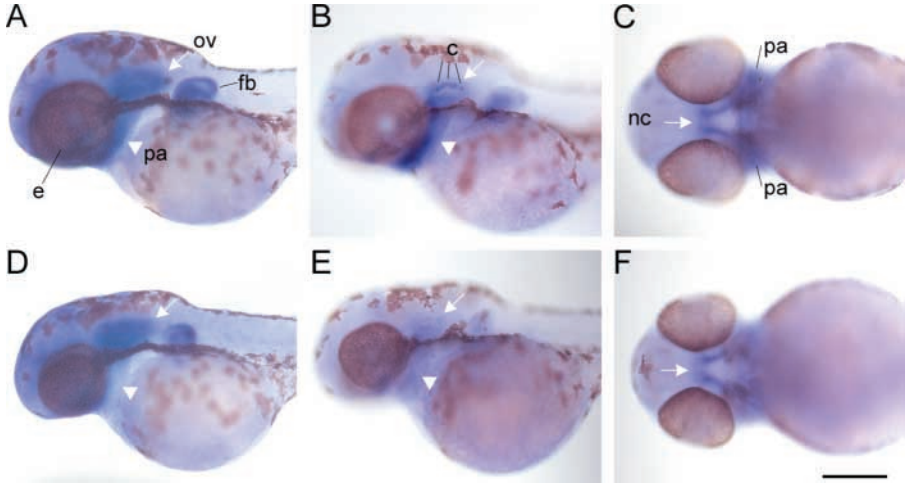

Fig. 8. In situ analysis of cartilage differentiation in *dfna5* morphants. (A,D) Lateral view of *col2a1* expression at 55 hpf. White arrows indicate the otic vesicle; white arrowheads indicate pharyngeal arches. Expression in the morphant otic vesicle (D) is unaffected compared with wild type (A). (B,C,E,F) *ugdh* expression in wild-type (B,C) and morphant (E,F) 55 hpf embryos. (B,E) Lateral view. (E) Expression in the developing morphant ear columns (indicated on wild type) and pharyngeal arches (white arrowhead) is reduced compared with wild-type (B). (C,F) Ventral view of expression in the developing neurocranium reveals no difference between wild-type and morphant embryos (arrows in C and F). Scale bar: 200 μm. c, column; e, eye; fb, fin bud; nc, neurocranium; ov, otic vesicle; pa, pharyngeal arches.

Discussion

DFNA5 plays a crucial role in hearing as its loss of function leads to a progressive form of dominant inherited hearing loss in humans. Despite a role in deafness, little is known about the biological function of DFNA5. Using reverse genetics in zebrafish, we found that *dfna5* is required for normal development of the ear.

dfna5 is essential for semicircular canal formation in the inner ear and cartilage formation in the jaw

During development of the inner ear, three projections emerge from the epithelium lining the otic vesicle (Haddon and Lewis, 1996; Waterman and Bell, 1994). These projections or epithelial columns then grow towards the center of the otic vesicle where they fuse and form the rudiments of the three semicircular canals. In larvae injected with either ATG or GT-MOs directed against *dfna5*, the columns fail to fuse. Instead, they appear as short and thickened masses, with a loss of an epithelial monolayer. As judged by thick sections, the number of cells is not reduced, but rather the space in between cells is increased. This phenotype suggests that these cells were unable to coordinate their movements to form elongated columns.

An additional phenotype occurs in animals injected with the ATG-MO that is predicted to mimic a loss-of-function allele. The pharyngeal cartilage is reduced in size and distorted. The cells stain weakly with Alcian Blue, suggesting that cartilage differentiation and production of the cartilage-specific extracellular matrix is disrupted. During differentiation, chondrocytes express high levels of collagens. Our results indicate that a collagen highly expressed by chondrocytes, *col2a1*, is reduced in *dfna5* morphants, suggesting that *dfna5* is required for differentiation of chondrocytes.

The role of HA in the developing ear

The phenotype seen in *dfna5* morphants is similar to the phenotype observed in zebrafish *jekyll* mutants (Neuhauss et al., 1996). These loss-of-function mutants have short and thickened epithelial columns that fail to elongate and fuse and cartilage differentiation is also affected. The *jekyll* gene encodes Ugdh, an enzyme necessary for the production of the dissaccharide unit of HA (Walsh and Stainier, 2001). Based on the similar phenotypes, we hypothesized that *dfna5* may be involved in the *ugdh* pathway. In MO-injected animals, we find that loss of *dfna5* function leads to loss of *ugdh* expression in the ear and the developing pharyngeal arches. We also find that HA is reduced in the developing semicircular canals of the *dfna5* morphants. Moreover, loss of HA is associated with reduced levels of *col2a1* expression, affecting differentiation of the branchial cartilage. By contrast, *col2a1* expression in morphant ears is normal, supporting our hypothesis that loss of *ugdh* in the developing ear is not affecting differentiation of

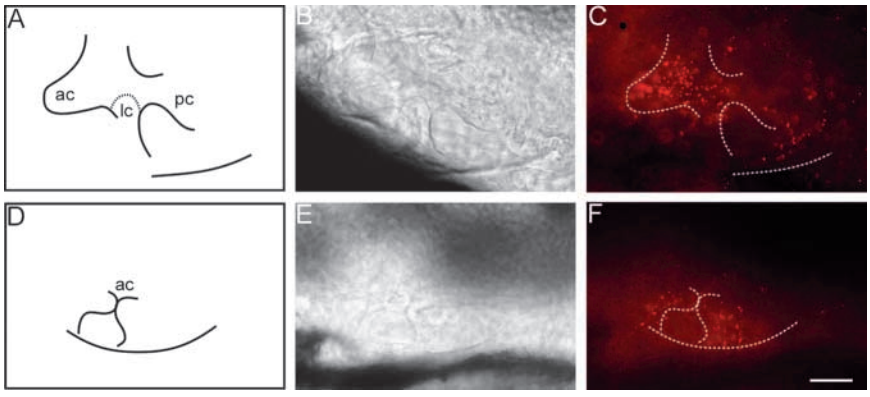

Fig. 9. Reduction of hyaluronic acid (HA) in the developing semicircular canals in *dfna5* morphants (54 hpf larvae). (A,D) Outline of the structures in a dorsolateral view of wild-type (B,C) and *dfna5* ATG-MO injected larval ears (E,F). The differential interference contrast (DIC) and corresponding fluorescent images are focussed at the level of the anterior column. An outgrowing protrusion of the anterior column (ac) in the wild-type ear (B) is filled with HA as shown by staining with biotinylated HA-binding protein (C). The lateral (lc) and posterior columns (pc) are out of focus in C. HA is reduced in both protrusions of the anterior column in a *dfna5* ATG-MO injected larval ear (E,F). Scale bar: 35 mm.

the ear cavity, but only the directed outgrowth of the canal projections.

In the ear, HA has been shown to play a role in the outgrowth of projections that fuse to form columns (Haddon and Lewis, 1991). HA is made of variable numbers of disaccharide units capable of forming filaments up to several micrometers in length. In the growing columns, epithelial cells at the tip of each protrusion are thought to secrete these long molecules that can act as a 'propellant'. Secretion of HA by a subset of cells within the projection may provide a driving force for growth in a particular direction. When HA is enzymatically removed in the epithelial columns, a similar phenotype of defective outgrowth is seen (Haddon and Lewis, 1991). In *dfna5* morphants, the reduction of HA levels results in an uncoordinated outgrowth of the epithelial projections. The epithelial cells are still proliferating, but the projection appears to lack the directional force of HA secretion by the cells at the leading edge. This causes disorganization of the epithelium as reflected by the missing basal lamina and stacking of cells. Controlled breakdown of the basal lamina underlying the outpocketing epithelium appears to be crucial for proper outgrowth. In wild-type canal projections, only the cells at the leading edge of the protrusion lack a basal lamina. In netrin 1 mouse mutants, the opposite situation is found: the basal lamina does not break down at all. However, this defect also results in unfused columns (Salminen et al., 2000), suggesting that only spatially and temporally correct remodeling of the basal lamina allows proper outgrowth and fusion of the epithelial projections.

Members of the protein family that share motifs with DFNA5 that are described in the literature are cancer-associated (Saeki et al., 2000; Thompson and Weigel, 1998; Lage et al., 2001; Watabe et al., 2001) (see http://www.sanger.ac.uk/cgi-bin/Pfam/getacc?PF04598 for DFNA5 family). This is particularly compelling because high levels of HA are a prognostic indicator for malignancy in clinical cases of human breast, ovarian and colon carcinomas. HA may promote invasiveness of cancer cells by providing a highly hydrated microenvironment that facilitates detachment and migration of cells (Toole, 2002). One possibility is that proteins of this family are able to regulate HA biosynthesis. All members of this protein family notably contain one (in the case of DFNA5) or more putative HA-binding sites. This motif is called BX_7B domain because it contains two basic amino acids (arginine or lysine) separated by seven non-acidic amino acids (Yang et al., 1994). This domain is found in all hyaladherins, proteins that interact with HA, such as aggrecan or CD44. Because this is a very common motif, it is not clear whether this domain is sufficient for binding to HA.

If Dfna5 regulates the HA biosynthetic pathway, it may act at the transcriptional level. Evidence for this notion is supported by a recent heterologous expression study in which human *DFNA5* was expressed in *S. pombe* cells (Gregan et al., 2003). Gregan and coworkers found a genetic interaction with the *S. pombe* gene *mcm10* (*cdc23*), which is involved in DNA replication. Interestingly, both DFNA5 and Mcm10p contain similar zinc-finger-like motifs that define the Mcm10 family of DNA replication proteins.

Human *DFNA5* hearing loss

How does our study add to the understanding of the human *DFNA5* disease? The anatomy of the vestibular inner ear, including the semicircular canals, is highly conserved among vertebrates (Riley and Phillips, 2003). Certain aspects of the development and morphogenesis of semicircular circular canals are similar. For example, in fish, frogs, birds and mammals, apposing epithelial walls or protrusions contact and fuse to form the rudiments of the semicircular canals (Haddon and Lewis, 1991; Martin and Swanson, 1993; Haddon and Lewis, 1996; Fekete et al., 1997). Development of the pharyngeal arches is also conserved among vertebrates (Graham, 2003). However, individuals with a mutation in *DFNA5* display neither obvious vestibular defects nor craniofacial malformations. Only one family has been found with a single mutation in *DFNA5* thus far. Whether the truncation of DFNA5 in humans results in haplo-insufficiency remains to be determined. Typically, only severe mutations such as null mutations cause syndromic hearing loss (Astuto et al., 2002). Syndromic deafness associated with craniofacial and/or skeletal deformations have been reported for three genes, *COL2A1*, *COL11A1* and *COL11A2* (reviewed by Morton, 2002). All three collagens are highly abundant in cartilage extracellular matrix (de Crombrugghe, 2001). Mutations in *COL11A2* cause syndromic as well as nonsyndromic hearing loss: congenital hearing loss is accompanied by various skeletal abnormalities in the case of Stickler syndrome (which can also be caused by mutations in *COL2A1* and *COL11A1*), whereas individuals with a mutation in *DFNA13* suffer from nonsyndromic progressive hearing loss at high and middle frequencies (Sirko-Osadsa, 1998; McGuirt et al., 1999; Kunst et al., 2000). The Marshall syndrome is associated with splicing mutations in *COL11A1* and characterized by craniofacial and skeletal abnormalities, cataracts and progressive sensorineural hearing loss. Computer tomography did not detect any malformations of ear bones. Therefore, hearing loss is thought to be due to direct effects on COL11A1 loss in the labyrinth and CNS (Griffith et al., 2000). In all three cases, genes affecting cartilage differentiation can cause progressive sensorineural hearing loss without causing cartilage malformations in the human ear.

This leads us to speculate that a complete loss of DFNA5 function in humans could cause cartilage phenotypes as seen in individuals with Stickler syndrome. Determination of the expression pattern of *Dfna5* in mammals will shed some light on this paradox. Nevertheless, HA is highly abundant in many areas of the developing human inner ear. It is suggested to serve there as a friction-reducing lubricant and molecular filter (Anniko and Arnold, 1995). If HA biosynthesis is reduced or lost in the ear, it is possible that this disruption of extracellular matrix causes increased mechanical stress on hair cells. This stress may lead to premature aging of hair cells and a progressive hearing loss, reminiscent of age-related hearing loss that also starts with high frequency sound.

References

Abdelhak, S., Kalatzis, V., Heilig, R., Compain, S., Samson, D., Vincent, C., Weil, D., Cruaud, C., Sahly, I., Leibovici, M. et al. (1997). A human homologue of the Drosophila eyes absent gene underlies branchio-oto-renal (BOR) syndrome and identifies a novel gene family. *Nat. Genet.* **15**, 157-164.

Ahmad, N. N., Ala-Kokko, L., Knowlton, R. G., Jimenez, S. A., Weaver, E. J., Maguire, J. I., Tasman, W. and Prockop, D. J. (1991). Stop codon

in the procollagen II gene (COL2A1) in a family with the Stickler syndrome (arthro-ophthalmopathy). *Proc. Natl. Acad. Sci. USA* **88**, 6624-6627.

Anniko, M. and Arnold, W. (1995). Hyaluronic acid as a molecular filter and friction-reducing lubricant in the human inner ear. *ORL J. Otorhinolaryngol. Relat. Spec.* **57**, 82-86.

Bitner-Glindzicz, M. and Tranebjaerg, L. (2000). The Jervell and Lange-Nielsen syndrome. *Adv. Otorhinolaryngol.* **56**, 45-52.

de Crombrugghe, B., Lefebvre, V. and Nakashima, K. (2001). Regulatory mechanisms in the pathways of cartilage and bone formation. *Curr. Opin. Cell Biol.* **13**, 721-727.

Fekete, D. M., Homburger, S. A., Waring, M. T., Riedl, A. E. and Garcia, L. F. (1997). Involvement of programmed cell death in morphogenesis of the vertebrate inner ear. *Development* **124**, 2451-2461.

Graham, A. (2003) Development of the pharyngeal arches. *Am. J. Med. Genet.* **119A**, 251-256.

Gregan, J., van Laer, L., Lieto, L. D., van Camp, G. and Kearsey, S. E. (2003). A yeast model for the study of human DFNA5, a gene mutated in nonsyndromic hearing impairment. *Biochim Biophys Acta*. **1638**, 179-186.

Griffith, A. J., Gebarski, S. S., Shepard, N. T. and Kileny, P. R. (2000). Audiovestibular phenotype associated with a COL11A1 mutation in Marshall syndrome. *Arch. Otolaryngol. Head Neck Surg.* **126**, 891-894.

Haddon, C. M. and Lewis, J. H. (1991). Hyaluronan as a propellant for epithelial movement: the development of semicircular canals in the inner ear of Xenopus. *Development* **112**, 541-550.

Haddon, C. and Lewis, J. (1996). Early ear development in the embryo of the zebrafish, Danio rerio. *J. Comp. Neurol.* **365**, 113-128.

Kimmel, C. B., Miller, C. T. and Moens, C. B. (2001). Specification and morphogenesis of the zebrafish larval head skeleton. *Dev. Biol.* **233**, 239-257.

Knudson, C. B. and Knudson, W. (2001). Cartilage proteoglycans. *Semin. Cell Dev. Biol.* **12**, 69-78.

Kunst, H., Huybrechts, C., Marres, H., Huygen, P., van Camp, G. and Cremers, C. (2000). The phenotype of DFNA13/COL11A2: nonsyndromic autosomal dominant mid-frequency and high-frequency sensorineural hearing impairment. *Am. J. Otol.* **21**, 181-187.

Lage, H., Helmbach, H., Grottke, C., Dietel, M. and Schadendorf, D. (2001). DFNA5 (ICERE-1) contributes to acquired etoposide resistance in melanoma cells. *FEBS Lett.* **494**, 54-59.

Leger, S. and Brand, M. (2002). Fgf8 and Fgf3 are required for zebrafish ear placode induction, maintenance and inner ear patterning. *Mech. Dev.* **119**, 91-108.

Liu, D., Chu, H., Maves, L., Yan, Y. L., Morcos, P. A., Postlethwait, J. H. and Westerfield, M. (2003). Fgf3 and Fgf8 dependent and independent transcription factors are required for otic placode specification. *Development* **130**, 2213-2224.

Magee, C., Nurminskaya, M. and Linsenmayer, T. F. (2001). UDP-glucose pyrophosphorylase: up-regulation in hypertrophic cartilage and role in hyaluronan synthesis. *Biochem. J.* **360**, 667-674.

Maroon, H., Walshe, J., Mahmood, R., Kiefer, P., Dickson, C. and Mason, I. (2002). Fgf3 and Fgf8 are required together for formation of the otic placode and vesicle. *Development* **129**, 2099-2108.

Martin, P. and Swanson, G. J. (1993). Descriptive and experimental analysis of the epithelial remodellings that control semicircular canal formation in the developing mouse inner ear. *Dev. Biol.* **159**, 549-558.

McGuirt, W. T., Prasad, S. D., Griffith, A. J., Kunst, H. P., Green, G. E., Shpargel, K. B., Runge, C., Huybrechts, C., Mueller, R. F., Lynch, E. et al. (1999). Mutations in COL11A2 cause non-syndromic hearing loss (DFNA13). *Nat. Genet.* **23**, 413-419.

Morton, C. C. (2002). Genetics, genomics and gene discovery in the auditory system. *Hum. Mol. Genet.* **11**, 1229-1240.

Neuhauss, S. C., Solnica-Krezel, L., Schier, A. F., Zwartkruis, F., Stemple, D. L., Malicki, J., Abdelilah, S., Stainier, D. Y. and Driever, W. (1996). Mutations affecting craniofacial development in zebrafish. *Development* **123**, 357-367.

Petit, C., Levilliers, J. and Hardelin, J. P. (2001). Molecular genetics of hearing loss. *Annu. Rev. Genet.* **35**, 589-646.

Piotrowski, T., Schilling, T. F., Brand, M., Jiang, Y. J., Heisenberg, C. P., Beuchle, D., Grandel, H., van Eeden, F. J., Furutani-Seiki, M., Granato, M. et al. (1996). Jaw and branchial arch mutants in zebrafish II: anterior arches and cartilage differentiation. *Development* **123**, 345-356.

Riley, B. B. and Phillips, B. T. (2003). Ringing in the new ear: resolution of cell interactions in otic development. *Dev. Biol.* **261**, 289-312.

Saeki, N., Kuwahara, Y., Sasaki, H., Satoh, H. and Shiroishi, T. (2000). Gasdermin (Gsdm) localizing to mouse Chromosome 11 is predominantly expressed in upper gastrointestinal tract but significantly suppressed in human gastric cancer cells. *Mamm. Genome* **11**, 718-724.

Salminen, M., Meyer, B. I., Bober, E. and Gruss, P. (2000). Netrin 1 is required for semicircular canal formation in the mouse inner ear. *Development* **127**, 13-22.

Schilling, T. F. and Kimmel, C. B. (1994). Segment and cell type lineage restrictions during pharyngeal arch development in the zebrafish embryo. *Development* **120**, 483-494.

Schilling, T. F. and Kimmel, C. B. (1997). Musculoskeletal patterning in the pharyngeal segments of the zebrafish embryo. *Development* **124**, 2945-2960.

Schilling, T. F., Piotrowski, T., Grandel, H., Brand, M., Heisenberg, C. P., Jiang, Y. J., Beuchle, D., Hammerschmidt, M., Kane, D. A., Mullins, M. C. et al. (1996). Jaw and branchial arch mutants in zebrafish I: branchial arches. *Development* **123**, 329-344.

Sirko-Osadsa, D. A., Murray, M. A., Scott, J. A., Lavery, M. A., Warman, M. L. and Robin, N. H. (1998). Stickler syndrome without eye involvement is caused by mutations in COL11A2, the gene encoding the alpha2(XI) chain of type XI collagen. *J. Pediatr.* **132**, 368-371.

Spicer, A. P., Kaback, L. A., Smith, T. J. and Seldin, M. F. (1998). Molecular cloning and characterization of the human and mouse UDP-glucose dehydrogenase genes. *J. Biol. Chem.* **273**, 25117-25124.

Thisse, C., Thisse, B., Schilling, T. F. and Postlethwait, J. H. (1993). Structure of the zebrafish snail1 gene and its expression in wild-type, spadetail and no tail mutant embryos. *Development* **119**, 1203-1215.

Thompson, D. A. and Weigel, R. J. (1998). Characterization of a gene that is inversely correlated with estrogen receptor expression (ICERE-1) in breast carcinomas. *Eur. J. Biochem.* **252**, 169-177.

Toole, B. P. (2001). Hyaluronan in morphogenesis. *Semin. Cell Dev. Biol.* **12**, 79-87.

Van Laer, L., Huizing, E. H., Verstreken, M., van Zuijlen, D., Wauters, J. G., Bossuyt, P. J., van de Heyning, P., McGuirt, W. T., Smith, R. J., Willems, P. J. et al. (1998). Nonsyndromic hearing impairment is associated with a mutation in DFNA5. *Nat. Genet.* **20**, 194-197.

Walsh, E. C. and Stainier, D. Y. (2001). UDP-glucose dehydrogenase required for cardiac valve formation in zebrafish. *Science* **293**, 1670-1673.

Watabe, K., Ito, A., Asada, H., Endo, Y., Kobayashi, T., Nakamoto, K., Itami, S., Takao, S., Shinomura, Y., Aikou, T. et al. (2001). Structure, expression and chromosome mapping of MLZE, a novel gene which is preferentially expressed in metastatic melanoma cells. *Jpn. J. Cancer Res.* **92**, 140-151.

Waterman, R. E. and Bell, D. H. (1984). Epithelial fusion during early semicircular canal formation in the embryonic zebrafish, Brachydanio rerio. *Anat. Rec.* **210**, 101-114.

Yang, B., Yang, B. L., Savani, R. C. and Turley, E. A. (1994). Identification of a common hyaluronan binding motif in the hyaluronan binding proteins RHAMM, CD44 and link protein. *EMBO J.* **13**, 286-296.